JOURNAL OF MATERIALS SCIENCE 22 (1987) 3566–3570

Quantitative XRD analysis of zirconia-toughened alumina ceramics

R. FILLIT, P. HOMERIN, J. SCHAFER, H. BRUYAS, F. THEVENOT
Ecole Nationale Supérieure des Mines, 42023 Saint-Etienne Cedex 2, France

An equation is proposed to give, from XRD data, the tetragonal to monoclinic phase ratio of zirconia in a toughened alumina ceramic material. Using several X-ray wavelengths, with different depths of penetration, quantitative analyses of the tetragonal to monoclinic phase ratio of zirconia as a function of depth were performed, on an as-sintered sample as well as on treated specimens. The phase transformations of zirconia at the surface and in the bulk of the material due to these treatments are discussed

1. Zirconia toughening of ceramics

Ceramic materials exhibit many properties (such as hardness, chemical stability, high-temperature mechanical properties) which allow the consideration of their use in structural applications instead of metallic alloys. Nevertheless, their development has been greatly limited because of their brittleness. One of the methods proposed in order to overcome this problem is the synthesis of particle composite materials [1, 2]. Adding a zirconia particle dispersion to ceramic materials, under specific conditions, allows enhancement of their mechanical behaviour [3]: strengthening and toughening, increase of crack initiation and growth energy, development of surface or bulk residual stresses.

Zirconia exhibits three well-defined polymorphs: the cubic and tetragonal crystallographic phases at high temperatures and the monoclinic phase at room temperature [4]. Nevertheless, the temperature at which the tetragonal to monoclinic transformation occurs depends on the particle size; it may not occur, even at room temperature, if the zirconia particles are small enough.

The martensitic tetragonal to monoclinic zirconia allotropic transformation is the basis of several different toughening mechanisms [5, 6] such as: microcracking at the tip of the crack; stress-induced phase transformation; compressive stresses in near-surface layers; interaction between the crack and zirconia particles.

A thermomechanical analysis of the toughening mechanisms shows the tetragonal to monoclinic transformation temperature decreases as the compressive stresses exerted by the surrounding matrix on the metastable zirconia particles is increased [7]. The toughening of an alumina ceramic matrix is thus especially significant: indeed, the elastic modulus of alumina (Young's modulus, $E = 400\,\mathrm{GPa}$) is approximately twice that of zirconia.

Quantitative analysis of tetragonal metastable and monoclinic stable zirconia contents, at the surface and in the bulk of the material, is thus especially interesting in order to understand the toughening mechanisms. The following sections explain how such analyses were performed, using different X-ray wavelengths, on a zirconia-toughened alumina material subjected to different treatments.

2. Sample preparation

An alumina material containing 15 vol % unstabilized zirconia (A15Z) was synthesized from the dissociation of an organic salt of zirconium. This method allows the production of the necessary fine and homogeneous zirconia dispersion required for effective toughening of a ceramic material [8].

An alumina (A6Z, Criceram, Jarrie, France) slurry was prepared in an aqueous solution of a zirconium soluble salt (acetate) (Magnesium Elektron, Manchester, UK). Upon heating of the slurry, zirconium salt dissociated into the hydroxide (gelification stage). The mixture was dried and calcined for 4 h at 800° C in order to transform the zirconium hydroxide into zirconia. The powder was then dry milled and hot pressed (1400° C, 15 min, 20 MPa) [9].

The densified material exhibits a flexural strength (σ_F) of 630 ± 35 MPa (three-point bending test) and a toughness (K_{Ic}) of 5.5 ± 0.3 MPa m$^{1/2}$ (SENB). The untoughened material exhibits a σ_F of 590 ± 55 MPa and a K_{Ic} of 3.8 ± 0.1 MPa m$^{1/2}$.

XRD analyses of the zirconia crystallographic phases were performed on an as-sintered sample as well as on surface- and bulk-treated specimens. The different treatments (Table I) were chosen for their representation of the different stages of processes usually followed during the manufacture of ceramic parts. These different treatments influence the tetragonal to monoclinic transformation of zirconia inclusions at the surface and/or in the bulk and thus the

TABLE I Types of treatment performed on the samples

Sample	Type of treatment	Conditions
A	As-sintered pellet	1400° C, 15 min, 20 MPa
B	A + severe grinding	Machining using diamond tools
C	B + careful polishing	Diamond paste (1 μm)
D	C + thermal ageing	1450° C, 1 h

0022–2461/87 $03.00 + .12

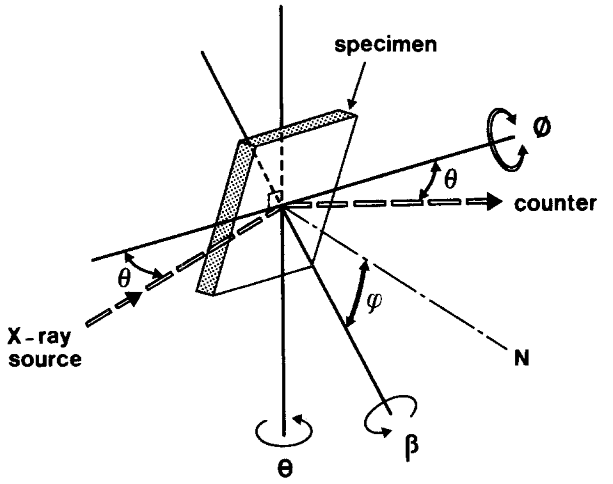

Figure 1 Principle of the equipment: θ, goniometer rotation axis; β, specimen rotation axis; ϕ, specimen tilting axis; N, line bisecting incident and refracted X-ray beams.

mechanical behaviour of the material. For this reason it is very important to know the ratio of tetragonal to monoclinic zirconia phases as a function of depth in the sintered materials.

3. Quantitative analysis of the tetragonal to monoclinic phase ratio of zirconia by XRD

3.1. Experimental technique

The equipment consists of a conventional X-ray powder diffractometer in combination with a specially designed and automatically computer-controlled specimen holder, the DOSOPHATEX (trade mark Courbon, S.A., F 42100, Saint-Etienne) [10, 11]. With the aid of this device the specimen is rotated (movement β) and tilted (movement ϕ) in addition to the conventional θ–2θ scanning movement (Fig. 1). First, when the diffraction spectrum is stored, during θ–2θ exploration, the pole figure of the specimen is integrated for ϕ from 0 to 60° for each θ position; using this method a large reduction is obtained in the texture effects on the sample because a greater amount of crystallites in the specimen is brought into the Bragg condition and all contribute to the intensity of the measured reflection $(h\,k\,l)$.

Second, to increase the accuracy of the X-ray measurement, the spectrum previously recorded can be corrected, to take into account the defocusing, absorption and geometrical phenomena due to the rotating and tilting movements. A correction factor [11, 12] for these secondary effects, f^{c}_{hkl} is calculated for each integrated line intensity $I(h\,k\,l)$, i.e. the curve $I(h\,k\,l)(\phi)$ is recorded. This is the mean intensity less the continuous background measured at the peak of the line $(h\,k\,l)$ when the specimen is tilted at an angle ϕ and has completed an integral number of rotations. The same measurement is performed with a random specimen $I^{r}(h\,k\,l)(\phi)$ of the same material and identical shape. Then, f^{c}_{hkl} is the ratio of integral $I(h\,k\,l)(\phi)$ corrected with $I^{r}(h\,k\,l)(\phi)$. With these secondary corrections, the texture effects are neutralized.

TABLE II Mass absorption coefficients of the different phases of the samples as a function of X-ray wavelengths and calculation of the penetration depths of rays

		Mo*K*α	Cu*K*α	Co*K*α	Cr*K*α
μ/ϱ ZrO_2	($cm^2\,g^{-1}$)	13.228	104.13	156.21	304.73
μ/ϱ Al_2O_3	($cm^2\,g^{-1}$)	3.21	31.78	49.25	101.13
μ/ϱ A15Z	($cm^2\,g^{-1}$)	5.27	46.70	71.31	143.11
τ	(μm)	23.32	5.69	4.34	2.74
z	(μm)	53.7	13.1	10.0	6.3

3.2. Procedure for phase analysis as a function of depth

The ability of X-rays to penetrate opaque substances is their most striking property. Nevertheless they are absorbed following the well-known equation:

$$I = I_0 \exp\left(\frac{-\mu\varrho x}{\varrho}\right)$$

where I_0 is the original beam intensity, I is the intensity transmitted after a path of length x in the material, ϱ is the density of the material, μ/ϱ is the mass absorption coefficient of the material.

As μ largely depends on the wavelength of the X-rays, the quantitative analysis of zirconia phases was made as a function of depth using Cr*K*α, Co*K*α, Cu*K*α, Mo*K*α radiations (Table II).

3.3. Quantitative analysis of the tetragonal to monoclinic phase ratio of zirconia

Quantitative analysis of cubic and monoclinic as well as tetragonal and monoclinic zirconia mixtures is reported by several authors [13–17]. As done by Porter and Heuer [15], use was made of an equation giving the intensity $I(h\,k\,l)_i$ of a diffraction line $(h\,k\,l)$ of a phase (i) for a volume fraction V_i of this phase in a mixture:

$$I(h\,k\,l)_i = K\frac{R(h\,k\,l)_i V_i}{2\mu_M}$$

where K is a constant independent of the diffracting substance but dependent on type of radiation used and beam size, V_i is the volume fraction of phase (i) in the mixture, μ_M is the linear absorption coefficient of the mixture, and R_i is given by:

$$R_i = \frac{1}{v_i^2}\left[|F_i|^2 P_i \underbrace{\left(\frac{1+\cos^2 2\theta_i}{\sin^2\theta_i \cos\theta_i}\right)}_{L_{pi}}\right](e^{-2M_i})$$

where v_i is the volume of the unit cell, F_i is the structure factor, P_i is the multiplicity, L_{pi} is the Lorentz polarization factor, θ_i is the Bragg angle, and e^{-2M_i} is the temperature factor (a function of θ).

In order to perform a precise analysis of a mixture of monoclinic and tetragonal zirconia, the $(1\,1\,\bar{1})_m$, $(1\,1\,1)_t$ and $(1\,1\,1)_m$ lines were taken into account. The monoclinic zirconia volume fraction with respect to the total volume of zirconia is given by the equation:

$$X_m = \frac{V_m}{V_m + V_t} = \frac{C[I(1\,1\,\bar{1})_m + I(1\,1\,1)_m]}{C[I(1\,1\,\bar{1})_m + I(1\,1\,1)_m] + I(1\,1\,1)_t}$$

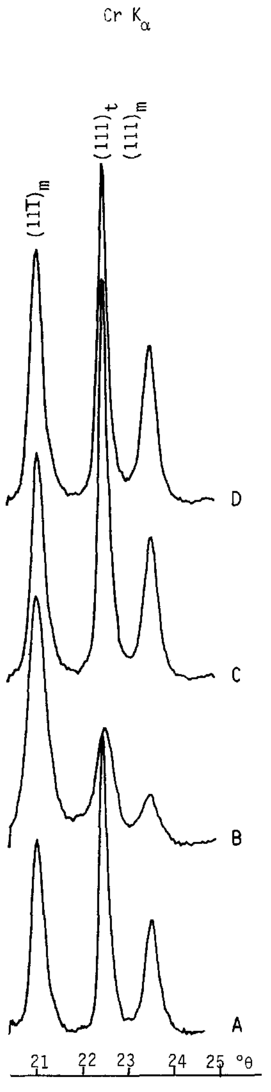

Figure 2 CrKα patterns of zirconia for the different types of treatment; conventional analysis without tilting showing texture of the samples.

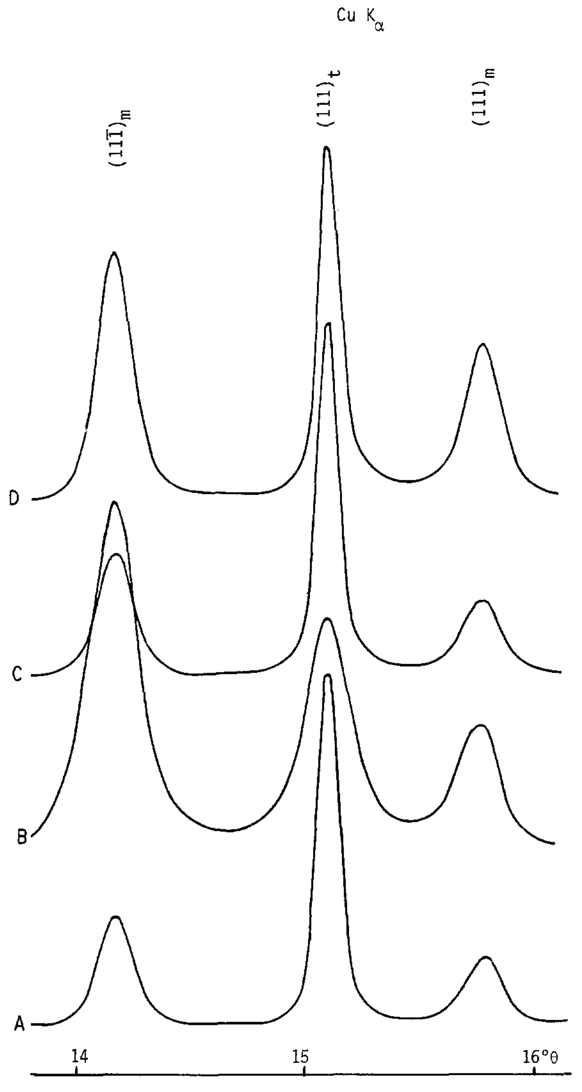

Figure 3 CuKα patterns of zirconia for the different types of treatment; conventional analysis without tilting showing texture of the samples.

with

$$C = R(1\,1\,1)_t/[R(1\,1\,\bar{1})_m + R(1\,1\,1)_m].$$

Structure factors were determined using Smith and Newkirk [18] data on the ion positions for the monoclinic phase of zirconia, and Teufer [19] data for the tetragonal phase.

Pattern fitting, using Fourier analysis, was carried out to determine the integrated intensity of $I(h\,k\,l)_i$ diffraction lines. This was especially useful when MoKα radiations were used because patterns presented line overlapping.

4. Results and discussion

Figs 2 and 3 show, for example, the $(1\,1\,\bar{1})_m$, $(1\,1\,1)_t$ and $(1\,1\,1)_m$ lines of the CrKα and CuKα diffraction patterns of the four samples. Fig. 4 gives an example of a more complete CoKα diffraction pattern showing the tetragonal and monoclinic zirconia as well as the α-alumina lines.

TABLE III Theoretical line intensities of zirconia $R(h\,k\,l)_i$ and the equivalent C coefficients as a function of X-ray wavelengths

	MoKα	CuKα	CoKα	CrKα
$R(1\,1\,\bar{1})_m$	346.35	81.58	59.51	34.52
$R(1\,1\,1)_m$	248.36	58.94	42.92	24.51
$R(1\,1\,1)_t$	828.24	194.09	141.09	81.07
C	1.393	1.381	1.377	1.373

The theoretical intensities $R(h\,k\,l)_i$ of the considered diffraction lines and the related coefficients, C, were calculated for the different radiations used (Table III). The atomic scattering factors were calculated from data of Tables 2.2A and 2.3.1 of [20].

Taking into account the experimental equipment geometry (Fig. 1), the penetration depth (z) of X-rays, normal to the surface, is given as a function of XR intensities by the equation:

$$I = I_0 \exp\left(-2\frac{\mu}{\varrho}\varrho\frac{z}{\sin\theta\,\overline{\cos\phi}}\right)$$

where $2z/\sin\theta\,\overline{\cos\phi} = x$, or $I = I_0\exp(-z/\tau)$ where

$$\tau = \frac{\sin\theta\,\overline{\cos\phi}}{2\mu}$$

ϕ is the angle between the normal to the sample surface and a line bisecting incident and refracted X-ray beams. As ϕ is ($\pm 60°$), $\overline{\cos\phi} = 0.866$. τ and the penetration depth (z), for an attenuation $I/I_0 =$

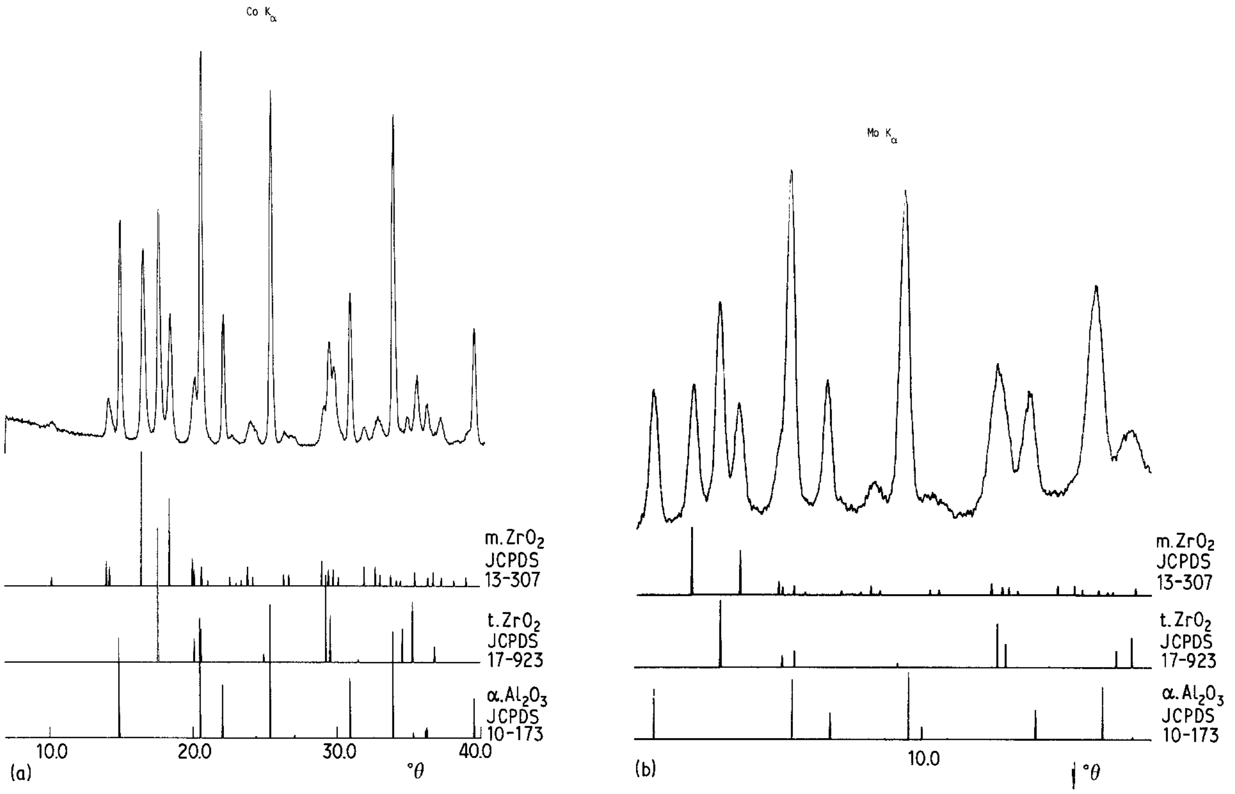

Figure 4 (a) Co$K\alpha$ pattern of alumina and zirconia (after thermal ageing) with rotation and tilting method (no texture effect). (b) Mo$K\alpha$ pattern of alumina and zirconia (as-sintered, A) with rotation and tilting method (no texture effect).

0.1, were calculated using the mass absorption coefficients of the considered atoms, as given by Table 2.1C of [20], for the determination of the A15Z mixture mass absorption coefficient.

Fig. 5 shows the variation of the monoclinic zirconia relative volume fraction (X_m) as a function of the analysis depth, for the four samples. As-sintered and polished samples show very similar values of X_m for all depths. The same surface tetragonal to monoclinic phase ratio, as on an as-sintered sample, can be restored after careful polishing of a machined sample if a thick layer (several tens of micrometres) is removed. On the other hand, severe grinding deeply disturbs the surface by inducing large tetragonal to monoclinic phase transformation ($X_m > 0.8$) and develops crystalline orientation texture (abnormal $I(1\,1\,\bar{1})_m - I(1\,1\,1)_m$ ratio).

Finally, the performed thermal ageing induced tetragonal to monoclinic zirconia phase transformation both at the surface and in the bulk of the material ($X_m = ct = 0.7$) due to grain coarsening (as revealed by microstructural analysis) and related to larger compressive stresses leading to a shift of $d(h\,k\,l)$ to lower values (Fig. 4 and Table IV).

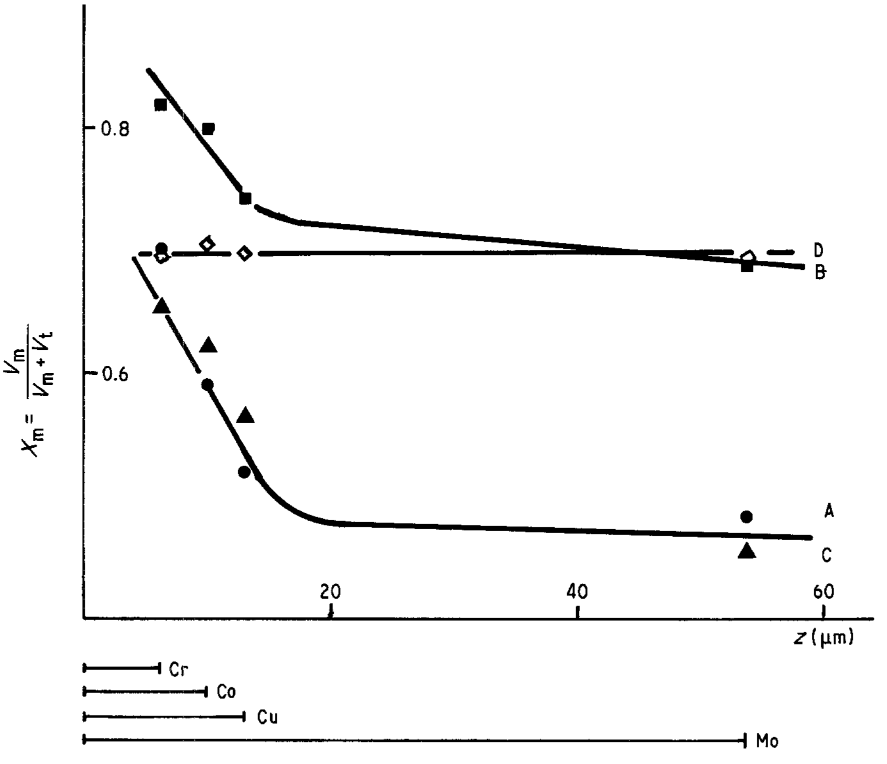

Figure 5 X_m as a function of X-ray penetration depth for the different types of treatment. Al_2O_3 + 15 vol % ZrO_2: (●) A, as-sintered; (■) B, machined; (▲) C, polished; (◇) D, thermally aged.

TABLE IV Relative change in the lattice parameters of the tetragonal and monoclinic zirconia lines after the different types of treatment (Cu$K\alpha$)

	d (JCPDS) (nm)	d (A–B) (nm)	d (A–C) (nm)	d (A–D) (nm)
$(1\,1\,\bar{1})_m$	0.316	0.000 66	0.000 98	0.001 00
$(1\,1\,1)_t$	0.296	0.000 77	0.000 77	0.000 86
$(1\,1\,1)_m$	0.2834	0.000 18	0.000 53	0.000 71

As reported by Kosmac [21], let us consider the zirconia phase transformation is homogeneous for $0 \leqslant z \leqslant a$ where the monoclinic relative volume fraction is X_{trans}. For $a \leqslant z \leqslant \infty$ it is X_{bulk}. a is given by the equation:

$$a = \ln\left[\frac{X_{\text{bulk}} - X_{\text{trans}}}{X_m - X_{\text{trans}}}\right]\tau$$

Table V gives the minimum transformation depth values calculated from this equation for $X_{\text{trans}} = 1$ and $X_{\text{bulk}} = 0.4$, using the measurements made with the different radiations used. This calculation method gives similar transformation depths for the as-sintered and polished samples ($a \geqslant 1.9\,\mu$m i.e. a few times the grain size). The machined sample shows a larger transformation depth ($a \geqslant 15\,\mu$m). The thermally aged sample shows both surface and bulk transformation of zirconia phases ($X_m = ct = 0.7$).

5. Conclusions

The use of the DOSOPHATEX and the XRD method proposed in this paper allowed the estimation of changes occurring in the phase ratio of zirconia as a function of depth after different treatments on a sintered zirconia toughened alumina.

The variation of the monoclinic to tetragonal zirconia phase ratio, between the surface and the bulk, is significant over a depth of only one to a few micrometres, i.e. a few times the grain size. After machining, major changes appear over a greater depth (more than 10 μm). Moreover, the surface appears highly texturated. Approximately the same zirconia phase ratio as in the case of the untreated sample can be restored after careful polishing, if a thick layer (several tens of micrometres) is removed. Important changes appear at the surface as well as in the bulk of the material after thermal ageing, which are due to grain coarsening leading to a drastic increase of the monoclinic zirconia volume fraction: $X_m = 0.7$ instead of less than 0.5 on an untreated sample.

Acknowledgement

The authors thank G. Orange, Insa, Lyon, France, for carrying out the mechanical testing.

Appendix: ion positions of zirconia

Monoclinic zirconia (after Smith and Newkirk [18])

Zr:	1.	(0.2758	0.0411	0.2082)
	2.	(0.7242	0.9589	0.7918)
	3.	(0.7242	0.5411	0.2918)
	4.	(0.2758	0.4589	0.7082)
O_I:	1.	(0.0703	0.3359	0.3406)
	2.	(0.9297	0.6641	0.6594)
	3.	(0.9297	0.8359	0.1594)
	4.	(0.0703	0.1641	0.8406)
O_{II}:	1.	(0.4423	0.7549	0.4789)
	2.	(0.5577	0.2451	0.5211)
	3.	(0.5577	0.2549	0.0211)
	4.	(0.4423	0.7451	0.9789)

TABLE V Minimum calculated depths of the tetragonal to monoclinic zirconia transformation as a function of the different types of treatment

	A	B	C	D
$a_{\min}$ (μm)	1.9	15.4	1.9	$\begin{cases} X_m = 0.7 = k \\ a = 0 \end{cases}$

Tetragonal zirconia (after Teufer [19])

Zr:	1.	(0	0	0)
	2.	(0.5	0.5	0.5)
O:	1.	(0	0.5	0.185)
	2.	(0.5	0	0.815)
	3.	(0	0.5	0.685)
	4.	(0.5	0	0.315)

References

1. A. G. EVANS, A. H. HEUER and D. L. PORTER, in Proceedings of the 4th International Conference on Fracture, ICF 4, Vol. 1, June 1977, edited by D. M. R. Taplin (Pergamon, Waterloo, Can., 1978) p. 529.
2. F. F. LANGE, in "Fracture Mechanics of Ceramics", edited by R. C. Bradt, A. G. Evans, D. P. H. Hasselman and F. F. Lange (Plenum, 1978) p. 799.
3. N. CLAUSSEN, in Proceedings of the European Colloquium on Ceramics in Advanced Energy Technology (D. Reidel, 1982) p. 51.
4. G. M. WOLTEN, *J. Amer. Ceram. Soc.* **46** (1963) 418.
5. N. CLAUSSEN and G. PETZOW, in "Energy and Ceramics", edited by P. Vincenzini (Elsevier, 1980) p. 680.
6. E. P. BUTLER, *Mater. Sci. Technol.* **1** (1985) 417.
7. F. F. LANGE, *J. Mater. Sci.* **17** (1982) 235.
8. D. W. SPRONSON and G. L. MESSING, *J. Amer. Ceram. Soc.* **67** (1984) C92.
9. J. P. BACH, P. HOMERIN, F. THEVENOT, G. ORANGE and G. FANTOZZI, presented at 6th CIMTEC, Milan, Italy, June 23–28, 1986, to be published.
10. R. FILLIT, H. BRUYAS, F. MARATRAY and A. POULALION, *Bull. Cercle d'Etudes des Métaux* **XV** (1) (1983) 1.
11. R. FILLIT and H. BRUYAS, XR Coll. Siemens, Grenoble (F), April 1985 (Siemens, 1985) p. 82.
12. F. MARATRAY, A. POULALION, R. FILLIT and H. BRUYAS, *Publ. Climax Molybdenum* (1984) M399E.
13. J. ADAM and B. COX, *J. Nucl. Energy* **A11** (1) (1959) 31.
14. R. C. GARVIE and P. S. NICHOLSON, *J. Amer. Ceram. Soc.* **55** (1972) 303.
15. D. L. PORTER and A. H. HEUER, *ibid.* **62** (1979) 298.
16. H. TORAYA, M. YOSHIMURA and S. SOMIYA, *ibid.* **67** (1984) C119.
17. P. A. EVANS, R. STEVENS and J. G. P. BINNER, *Brit. Ceram. Trans. J.* **83** (1984) 39.
18. D. K. SMITH and H. W. NEWKIRK, *Acta Cryst.* **18** (1965) 983.
19. G. TEUFER, *ibid.* **15** (1962) 1187.
20. J. A. IBERS and W. C. HAMILTON, International Table for XR Crystallography, Vol. 4 (Kynoch Press, Birmingham, UK, 1974).
21. T. KOSMAC, R. WAGNER and N. CLAUSSEN, *J. Amer. Ceram. Soc.* **64** (1981) C72.

Received 13 October 1986
and accepted 22 January 1987